

level is also related to DVT [17, 20] and is valuable, because measurements can be repeated easily and are quite sensitive to thrombotic events [5, 21–25]. The D-dimer value immediately increases at the onset of thrombotic events, so is one of the most reliable blood markers of VTE.

In this prospective study we tried to clarify the true incidence rate of VTE including asymptomatic occurrence, and the onset timing in patients with neuroepithelial tumor, and investigated the efficacy of combined D-dimer measurement and Doppler ultrasonography of the lower extremity for early detection of DVT to prevent fatal PE.

Clinical material and methods

Study population

Eighty-one consecutive patients with neuroepithelial tumor were prospectively enrolled in this study between July 2007 and December 2008. All patients were admitted for treatment, including surgical resection, biopsy, chemotherapy, or radiation therapy, at Tohoku University Hospital. Patients who underwent initial surgery in another hospital and were admitted for concomitant treatment were also included. Histological diagnosis was based on the World Health Organization (WHO) classification [26]. Patients with metastatic brain tumor, non-neuroepithelial tumor such as meningioma or germ cell tumor, and spinal cord tumor, and patients under the age of 18 years were excluded. Informed consent was obtained from each patient or guardian on admission and before computed tomography (CT) with contrast medium, or anticoagulant therapy.

Data collection and analysis

The following variables were prospectively recorded in a computerized data base for analysis: age, sex, lower extremity paresis, performance status at VTE occurrence, histological diagnosis (WHO grade), chemotherapy, and maximum serum D-dimer level. Neuroimaging findings, including CT, magnetic resonance (MR) imaging, and Doppler ultrasonography, were also recorded.

Protocol

The serum D-dimer measurements and Doppler ultrasonography were performed according to the following protocol. On admission, the serum D-dimer level was quantitatively measured in all patients. For patients who underwent surgery, including tumor resection and biopsy, it was measured within one week after surgical intervention and followed every week. Doppler ultrasonography of the

lower extremity was carried out two and five weeks after surgery, then every two weeks until discharge. For patients who did not undergo surgery, serum D-dimer level was measured every week and Doppler ultrasonography was carried out every two weeks. It is known that serum D-dimer level is sometimes elevated after surgery, even if there is no VTE, but the increase is rarely so high. Increased serum D-dimer level exceeding 10.0 $\mu\text{g/ml}$ elicited further examination for VTE by Doppler ultrasonography or CT with contrast medium of the chest, abdomen, and lower extremities (Fig. 1).

Doppler ultrasonography

Doppler ultrasonography was performed with SSA-770A (Toshiba Medical System, Otawara, Japan) or ProSound alpha10 (Aloka, Tokyo, Japan) equipment. The examination was performed in supine posture with a pillow placed beneath the knees. The diagnosis criterion for DVT was the inability to compress the veins in a cross-section (the primary basis for diagnosis). The presence of thrombus, the overall characteristics of the thrombus, absence of spontaneous venous flow, absence of respiratory phasicity, and absent or incomplete color filling signal, were adjuncts in assessment of the presence of thrombus. Dilation of the lower extremity veins or congestive venous flow was not regarded as DVT.

Clinical management

Elastic compression stockings were worn by all patients after admission for prophylaxis. Intermittent pneumatic compression was also used for all patients treated by surgery. Patients were mobilized after surgery as soon as

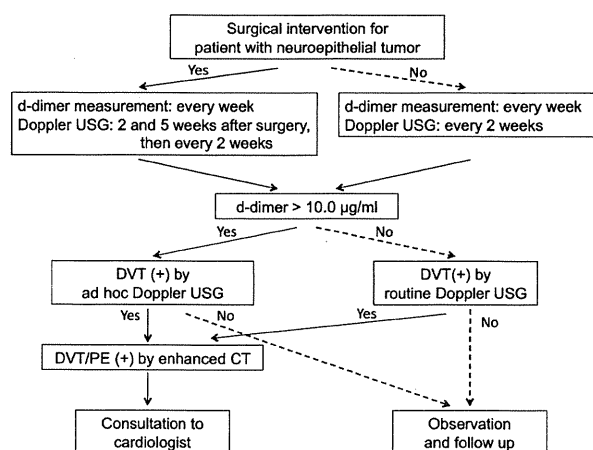


Fig. 1 Flow diagram showing the diagnosis of venous thromboembolism in patients with neuroepithelial tumor. CT, computed tomography; DVT, deep vein thrombosis; PE, pulmonary embolism; USG, ultrasonography

possible, usually from the day after surgery and, if necessary, physical therapy was started. Continuous heparin infusion or low molecular weight heparin was not administered. Patients were referred to the cardiology department if VTE was detected. If the thrombus extended proximal of the popliteal vein, unfractionated heparin was administered with or without filter placement on the inferior vena cava, followed by warfarin administration.

Statistical analysis

Differences in characteristics between patients with and without VTE were examined by Fisher’s exact test or Student’s *t* test. Probability values ≤0.05 were considered statistically significant.

Results

The characteristics of the 81 patients with neuroepithelial tumor are shown in Tables 1 and 2. Sixty-one (75.3%) patients underwent resection and 11 (13.6%) patients received stereotactic biopsy. Nine patients had previously undergone surgical treatment and histological diagnosis had been obtained. After surgery, 28 (34.6%) patients received concomitant radiation therapy and chemotherapy, 21 (25.9%) received chemotherapy only, and seven (8.6%) received radiation therapy only. Sixteen (19.8%) patients received neither radiation therapy nor chemotherapy after surgery. Nine patients did not undergo surgery during this period, three (3.7%) patients received chemotherapy and radiation therapy, three (3.7%) patients received

Table 2 Histological diagnosis of 81 patients

Histology	Number of patients
WHO grade IV	
Glioblastoma	38
Gliosarcoma	1
WHO grade III	
Anaplastic astrocytoma	8
Anaplastic oligodendroglioma	8
Anaplastic oligoastrocytoma	2
Gliomatosis cerebri	3
WHO grade II	
Diffuse astrocytoma	7
Oligodendroglioma	4
Oligoastrocytoma	1
Ependymoma	1
Pleomorphic xanthoastrocytoma	1
Glioneuronal tumor	1
WHO grade I	
Pilocytic astrocytoma	3
Ganglioglioma	3

chemotherapy only, and three (3.7%) patients received neither radiation therapy nor chemotherapy.

Incidence of VTE

During the follow-up period, VTE occurred in 12 (14.8%) patients (seven males and five females; age 34–75, mean 59.0 years) (Table 3). One patient who presented with loss

Table 1 Characteristics of 81 patients with neuroepithelial tumor with or without VTE

	Total	VTE	Non VTE	<i>P</i> value
Number of cases	81	12	69	
Age in years, min–max (mean)	24–78 (50.8)	34–75 (59.0)	24–78 (49.4)	0.038*
Male:female (% of females)	40:41 (50.6%)	7:5 (41.7%)	33:36 (52.2%)	0.5
Maximum value of D-dimer in µg/ml, mean ± SD	5.3 ± 6.3	14.5 ± 9.7	3.46 ± 3.6	<0.001*
Histology				
Grades I + II	6 + 15 (25.9%)	0 + 0 (0%)	6 + 15 (30.0%)	0.026*
Grades III + IV	21 + 39 (74.1%)	4 + 8 (100%)	17 + 31 (70.0%)	
Hemiparesis in the lower extremity				
MMT ≤2/5	16/81 (19.8%)	5/12 (41.7%)	11/69 (15.9%)	0.039*
MMT >3/5	65/81 (80.2%)	7/12 (58.3%)	58/69 (84.1%)	
Performance status (3–4)	31/81 (38.3%)	6/12 (50%)	25/69 (36.2%)	0.36
Corticosteroid therapy	27/81 (33.3%)	6/12 (50%)	21/69 (30.4%)	0.18
Surgery	72/81 (88.9%)	10/12 (83.3%)	62/69 (89.9%)	0.507
Radiation therapy	38/81 (46.9%)	7/12 (58.3%)	31/69 (44.9%)	0.390
Chemotherapy	55/81 (67.9%)	12/12 (100%)	43/69 (62.3%)	0.012*

MMT manual muscle test, SD standard deviation, VTE venous thromboembolism

* Statistically significant

of consciousness during rehabilitation was the only symptomatic case (Case 3) whereas 11 patients identified by screening for VTE were without symptoms. Ultrasonography and CT of the chest, abdomen, and lower extremities identified isolated DVT in nine (11.1%) patients and combined DVT and PE in three (3.7%) patients. Three of the nine patients with isolated DVT had DVT extending to the popliteal vein (Cases 1, 4, and 9), and were treated with anticoagulant therapy. The two patients with asymptomatic PE (Cases 2 and 6) were treated with anticoagulant therapy and one symptomatic patient with PE (Case 3) was treated with inferior vena cava filter placement and anticoagulant therapy. During this period, no death caused by PE occurred (Figs. 2, 3).

To determine the risk factors for VTE, we analyzed the correlations between clinical data and development of VTE. The patients were classified into two groups—patients with and without VTE. Clinical data including age, sex, WHO grade, paresis of the lower extremity, performance status, administration of corticosteroids, surgery, radiation therapy, and chemotherapy were analyzed. Statistical analysis revealed that high age ($P = 0.038$), WHO grade III or IV (grades I and II vs. III and IV, $P = 0.026$), and presence of paresis in the lower extremity (manual muscle test 0–2 vs. 3–5, $P = 0.039$) were significant risk factors for VTE (Table 1). Chemotherapy was also a significant risk factor ($P = 0.012$), in fact, 11 of 12 patients with VTE were treated with temozolomide and one patient with VTE was treated with ACNU (1-(4-amino-2-methyl-5-pyrimidinyl) methyl-3-(2-chloroethyl)-3-nitrosourea hydrochloride). In contrast, sex, performance status, and corticosteroid administration had no statistical correlation with the development of VTE (Table 1).

Serum D-dimer level

Most patients had a low serum D-dimer level on admission (mean 1.06 $\mu\text{g/ml}$) and maintained this low level. The maximum D-dimer value during the observation period was significantly higher in patients with VTE than in those without VTE (14.5 ± 9.7 vs. 3.46 ± 3.6 $\mu\text{g/ml}$, $P < 0.001$). The elapsed time since surgery ranged between 1 and 103 days (Table 3). At first, additional examination with Doppler ultrasonography and/or CT with contrast medium were carried out for patients whose D-dimer level was over 10.0 $\mu\text{g/ml}$, which was observed for 12 of 81 patients (Fig. 4). We identified the cut-off value of serum D-dimer for detection of VTE as 5.4 $\mu\text{g/ml}$ (75th percentile), which gave 83% sensitivity (10 of 12 patients) and 84% specificity (58 of 69 patients) for detection of VTE. In VTE patients, D-dimer level was normalized with appropriate treatment. Other causes of serum D-dimer elevation, for example atrial fibrillation, sinus thrombosis, systemic malignant diseases, or hematological diseases were not observed for any patients.

Doppler ultrasonography findings and treatment

Doppler ultrasonography detected VTE in 12 of the 81 patients. VTE was detected with ad-hoc Doppler ultrasonography because of D-dimer elevation over 10.0 $\mu\text{g/ml}$ in six patients, and in the other six patients it was detected with regular scheduled (not ad-hoc) Doppler ultrasonography between D-dimer measurement intervals. Luminal thrombus was revealed in eight (66.7%) patients, organized thrombus in two (16.7%) patients, and floating thrombus in two (16.7%) patients. They were referred to the cardiology department and treated by cardiologists. Six patients received anticoagulant therapy for PE or DVT extending proximal to the popliteal vein. Serial Doppler ultrasonography showed total organization or regression of the thrombus in five of these six patients. In one patient, follow-up Doppler ultrasonography was not conducted, but no recurrent PE or death occurred. The other six patients were observed without anticoagulant therapy because the thrombus was found to be distal DVT. During the observation period, follow-up Doppler ultrasonography showed thrombus regression and organization in three and two patients, respectively. No thrombus extension was observed, although in one patient follow-up Doppler ultrasonography was not performed. No death or symptomatic VTE was observed during the observation period (Table 3). For the 12 patients, newly detected neurological deficit or other systemic symptoms after VTE diagnosis were not observed at discharge.

Duration of follow-up period

Doppler ultrasonography and serum D-dimer measurements were monitored until discharge for all patients. The median length of hospital stay was 123 days (range, 8–634 days). Patients were then followed up in the outpatient department with serum D-dimer measurements. During the follow-up period, 42 (51.9%) patients died of tumor progression. However, no VTE occurred. The median length of follow up from the initial surgery was 600 days (range, 23–1,361 days).

Discussion

Previous studies of VTE incidence were based on retrospective data analysis [8, 9, 27, 28]. The diagnosis of VTE depended on presentation with symptoms, for example leg swelling or PE. In general, PE may cause sudden death, so that early detection before symptomatic manifestation is desirable. We previously reported a retrospective analysis of the incidence of symptomatic VTE in patients with malignant glioma as 1.9% [29]. In comparison, the incidence in this study is much higher, VTE occurred in 14.8% of patients with neuroepithelial tumor and PE occurred in

Table 3 Characteristics of the 12 patients with VTE

	Age (years), sex	Histology	Maximum D-dimer (µg/ml)	Days after surgery	Paresis		DVT		PE	Treatment		Follow-up Doppler ultrasonography
					Upper extremity	Lower extremity	Doppler ultrasonography of the lower extremity	Proximal extension		Anti-coagulants	IVC filter	
1	34, M	AG	16.3	^a	Rt.4/5	Rt.4/5	Luminal thrombus in Rt. popliteal vein and femoral vein	Yes	None	Yes	None	Not examined
2	35, M	AOA	22.9	17	Lt.3/5	Lt.3/5	Luminal thrombus in Lt. popliteal vein and femoral vein	Yes	Yes asymptomatic	Yes	None	No thrombus
3	53, M	GB	27.5	46	Rt.1/5	Rt.2/5	Luminal thrombus in Rt. soleus vein and popliteal vein	Yes	Yes symptomatic ^b	Yes	Yes	No thrombus
4	56, F	GB	21.6	5	Rt.2/5 Lt.4/5	Rt.1/5 Lt.2/5	Floating embolus in bilateral popliteal veins	Yes	None	Yes	None	No thrombus
5	57, F	AA	6.9	103	Lt.1/5	Lt.1/5	Luminal thrombus in Lt. peroneus vein	None	None	None	None	No thrombus
6	59, M	AO	23.5	1	None	None	Luminal thrombus in Lt. soleus vein and popliteal vein	Yes	Yes asymptomatic	Yes	None	No thrombus
7	60, M	GB	2.1	1	Lt.4/5	Lt.4/5	Organized thrombus in Lt. soleus vein	None	None	None	None	Organized thrombus
8	65, F	GB	6.3	7	None	None	Luminal thrombus in Lt. anterior tibial vein	None	None	None	None	No thrombus
9	69, M	GB	3.2	23	None	None	Floating thrombus in Lt. soleus vein and popliteal vein	Yes	None	Yes	None	Organized thrombus
10	70, M	GB	27.5	6	Rt.3/5	Rt.2/5	Luminal thrombus in Rt. soleus vein and peroneus vein	None	None	None	None	Organized thrombus
11	75, F	GB	8.0	8	Rt.2/5	Rt.2/5	Luminal thrombus in Rt. soleus vein	None	None	None	None	No thrombus
12	75, F	GB	8.3	44	None	None	Organized thrombus in Lt. soleus vein Dilation of Lt soleus vein	None	None	None	None	Not examined

AA anaplastic astrocytoma, AG anaplastic ganglioglioma, AO anaplastic oligodendroglioma, AOA anaplastic oligoastrocytoma, DVT deep vein thrombosis, F female, GB glioblastoma, IVC inferior vena cava, Lt left, M male, PE pulmonary embolism, Rt right, VTE venous thromboembolism

^a Operated five years previously

^b Presented with loss of consciousness during rehabilitation

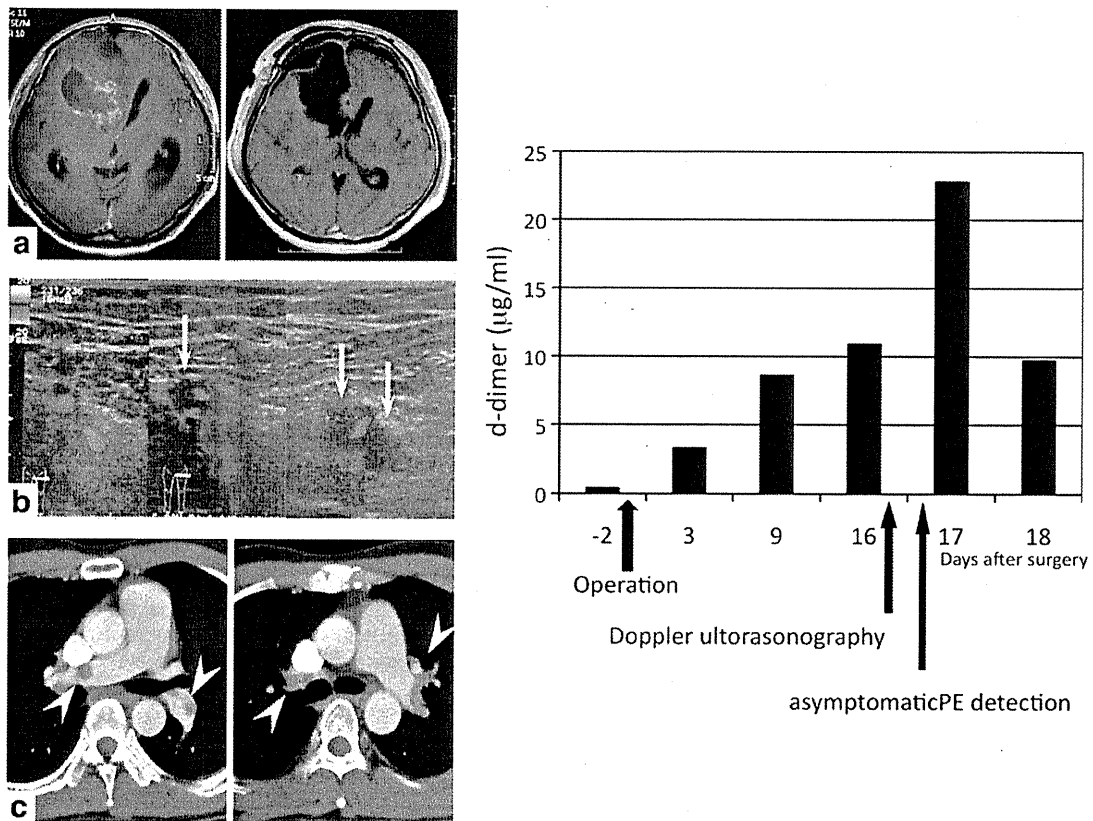


Fig. 2 Case 2. A 35-year-old male underwent gross total removal of right frontal anaplastic oligoastrocytoma (a, left panel: preoperative MR image, right panel: postoperative MR image). Postoperatively, he suffered slight left hemiparesis but was independent in daily life. Suddenly, D-dimer value elevated to 11.0 µg/ml 16 days after surgical resection. Doppler ultrasonograms showing luminal thrombus in the left

popliteal and femoral veins (b, arrows show the blood flow defect in the femoral vein). Next day, D-dimer value was further elevated to 22.9 µg/ml. CT scans with contrast medium showing thrombus in the bilateral pulmonary arteries with no clinical symptoms (c, arrowheads). He was referred to the cardiology department and treated with heparin/warfarin. The bar graph shows the sequential D-dimer values of this patient

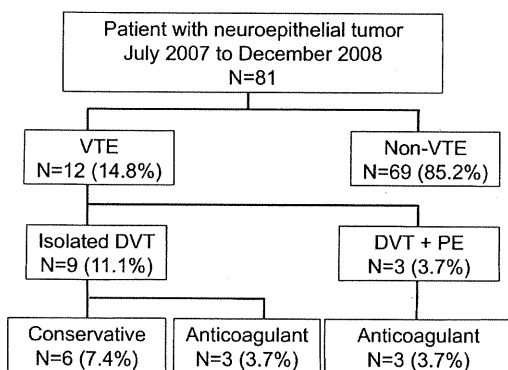


Fig. 3 Flow diagram showing the screening and treatment of 81 patients. Diagnosis of venous thromboembolism (VTE) was based on Doppler ultrasonography findings. DVT, deep vein thrombosis; PE, pulmonary embolism

3.7% of patients. One possible explanation of this discrepancy is the detection of asymptomatic VTE. In this study, only one patient (1.2%) presented with symptomatic

VTE (PE), a rate compatible with our previous report. One previous prospective study found the rate of VTE was 13% in patients after elective neurosurgery [7]. Brandes et al. also reported a prospective study which revealed a 20.8% risk of DVT in glioma patients 12 months after surgery [30]. Simanek et al. focused on symptomatic VTE occurrence in patients with high-grade glioma [31]. They treated high-grade glioma patients with low-molecular-weight heparin and a compression stocking for 10 days after surgery and reported 24% of patients showed symptomatic VTE (including nine PE). Compared with these, the duration of follow up was relatively short in our study, however, it covered the high-risk period of VTE [8]. The proportion of symptomatic VTE patients in this study was much lower than in the literature, despite not using anticoagulant therapy. This might also indicate the efficacy of our screening procedure for early detection of VTE before symptomatic manifestation.

The purpose of VTE treatment is to prevent PE, which sometimes causes cardiopulmonary arrest. Therefore, DVT

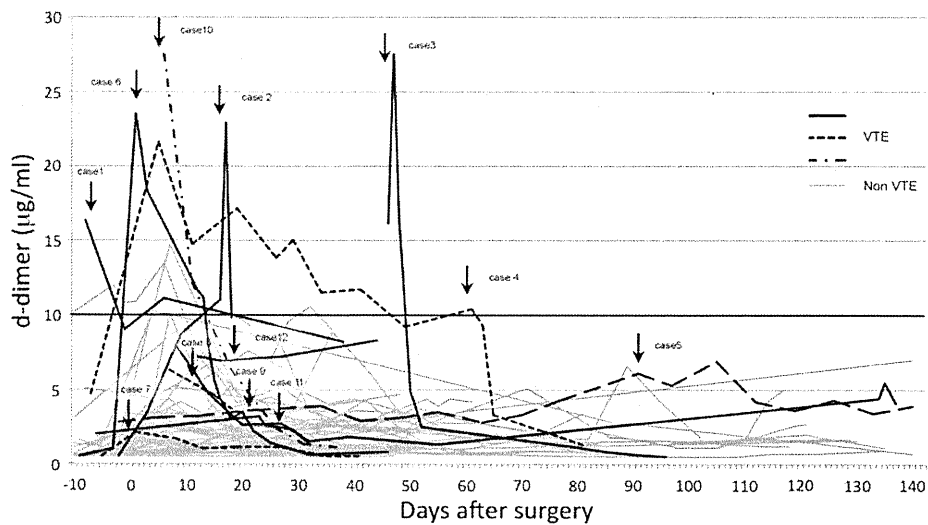


Fig. 4 Sequential D-dimer values of all patients. *Black lines (solid line, dashed line, and dash-dot line) and gray lines* indicate patients with venous thromboembolism (VTE) and without VTE, respectively. Case numbers as in Table 3. *Arrows* indicate VTE onset. The maximum D-dimer value was higher than 10.0 µg/ml for 12 patients. Although D-dimer level did not reach 10.0 µg/ml for most non-VTE patients, for patients with VTE D-dimer values were much higher. Note that D-dimer elevation occurred at random times after surgery. Case 1 underwent surgery previously and only chemotherapy was carried out during this period. For this patient, day 0 indicates the start day of chemotherapy. Case 10 lacked preoperative D-dimer data, because he underwent surgery in another hospital and was transported

must be detected before it becomes symptomatic and the appropriate treatment initiated. In this study, VTE was detected in 12 patients. Six of the 12 patients harbored venous thrombus extending to the popliteal vein, and all received anticoagulant therapy. Three of the six patients harbored PE, which is a high incidence, but the other three patients did not have symptomatic or asymptomatic PE, despite the presence of massive DVT. These three patients are extremely important examples of detection of patients at high risk of PE before symptom onset.

As shown in Table 1, the risk factors for VTE in this study were identified as the presence of paresis in the lower extremity, histological diagnosis (WHO grade), age, and use of chemotherapy, which are compatible with previous reports [3, 8, 29]. D-Dimer measurement is well recognized as a marker of recurrent VTE in patients without cancer [32–35]. Moreover, measurement of serum D-dimer level also effectively detects VTE in patients with ovarian, uterine, and breast cancer and brain tumor [32, 36, 37]. A prospective study revealed that D-dimer level could be used to predict the occurrence of VTE in patients with various cancers [32]. However, Doppler ultrasonography or CT to detect asymptomatic VTE was not performed, and objective imaging methods were used to confirm that the patient had developed symptoms of VTE. They concluded that

to our institution for further treatment. Preoperative serum D-dimer value was not available for Cases 8 and 12 also. Case 3 was the first case of this series. He suddenly presented with hypotension and a significant decrease in oxygen saturation during rehabilitation. He was diagnosed as symptomatic PE and DVT by Doppler ultrasonography of the lower extremity and CT with contrast medium of the chest. Serum D-dimer level was above 10.0 µg/ml. These findings show that sequential serum D-dimer level analysis is useful for detecting VTE. This figure indicated that patients with VTE certainly showed sudden elevation of serum D-dimer value and there is no optimum timing for Doppler ultrasonography

patients with elevated D-dimer level were at high risk of VTE. In comparison, our study showed that sequential D-dimer measurement was useful for screening for VTE, even in patients without elevated D-dimer level. In this study a D-dimer cutoff value of 5.4 µg/ml enabled identification of VTE with 83% sensitivity and 84% specificity. In addition, the test is easy to perform and enables close serial screening [24].

Doppler ultrasonography of the lower extremity is an efficient, less invasive method for screening for DVT in both symptomatic and asymptomatic patients [38–40]. In fact, Doppler ultrasonography findings varied widely in our patients, and included organized thrombus, luminal thrombus, floating thrombus, and congestive flow without thrombus or dilation of the deep vein. Although Doppler ultrasonography enables effective detection of DVT in patients with subarachnoid hemorrhage [10, 38], screening of all patients every week may be difficult, so this method may be secondary to general screening by D-dimer measurement. Various studies have tried to detect VTE in the early period to prevent lethal PE, but usually used non-invasive screening tests with low sensitivity, for example radioactive fibrinogen scanning or highly invasive methods such as venography and ventilation/perfusion scintigraphy [7, 41, 42]. Compared with these methods, our procedure is

not only less invasive but also provides higher sensitivity and specificity.

The method of D-dimer measurement is relatively easy to repeat and the serum D-dimer level increases immediately on VTE occurrence. However, the increased D-dimer level is indicative of a systemic thrombotic event without locational information. Isolated DVT and PE are hard to distinguish by measurement of serum D-dimer level. In contrast, Doppler ultrasonography can detect DVT directly, but is time-consuming and requires much manpower. Therefore, routine Doppler ultrasonography is not realistic for every patient. Moreover, it is hard to predict when VTE tends to occur. The first two months after surgery are the high-risk period for VTE in patients harboring glioma [8]. In this study, we decided to perform Doppler ultrasonography of the lower extremities two and five weeks after surgery, on the basis of the findings of their study, but D-dimer elevation occurred at random times after surgery (Fig. 4). This result indicates there is no optimum timing for Doppler ultrasonography, so it is not sufficient to follow up patients with Doppler ultrasonography only. In this study, no patient was followed up with Doppler ultrasonography only. Taken together, serial D-dimer measurement is regarded as the first-line screening method for VTE, followed by Doppler ultrasonography to detect DVT.

The efficacy of prophylactic heparin-based anticoagulant therapy is well recognized. Moreover, the complication of bleeding is also known to be one of the most miserable complications after neurological surgery [43, 44]. Collen et al. reviewed the literature, and performed a meta-analysis which showed the efficacy of anticoagulant therapy and the subsequent risk of bleeding. Although the study population was heterogeneous, bleeding complications, for example massive intracranial hemorrhages or minor bleeding, tend to occur in patients treated with anticoagulant. They also showed that prophylaxis with intermittent pneumatic compression was equally efficacious [43]. This means that heparin use might be limited for high-risk patients. In our study, heparin-based anticoagulant therapy was not performed for prophylaxis. However, when PE or DVT with proximal extension to the popliteal vein was detected, anticoagulant therapy was started immediately for VTE treatment. Our screening procedure gave the appropriate timing for starting anticoagulant therapy, which led to good results with no bleeding complication or low incidence of symptomatic VTE.

In our study, Doppler ultrasonography showed various venous findings. Which finding indicates the highest risk of PE remains controversial, but thrombus extending proximal to the popliteal vein is one of the risk factors of PE [40, 45]. Six patients harbored thrombus localized in the soleus, tibial, or peroneus vein. Because of the relatively low risk of PE, and potentially catastrophic bleeding complication,

they were not treated with heparin-based anticoagulant therapy. The natural history of isolated distal DVT is unknown and treatment of this entity is still controversial, but our patients were treated with mechanical prophylaxis and physical therapy, which can be one treatment option. In addition, close follow up with D-dimer measurement and Doppler ultrasonography was continued even five weeks or more after surgery, which resulted in total regression or organization in five of six patients and no PE onset (Table 1).

The combination of D-dimer measurement and Doppler ultrasonography is currently the most favorable procedure for early VTE detection, but no standardized measurement method or consensus for the normal range of D-dimer values has been established, so the cutoff value of 5.4 µg/ml in this study cannot be compared directly with previous findings. Sequential measurement of serum D-dimer level is definitely valuable for VTE screening, however [17].

Conclusions

This prospective study in Japan revealed that the occurrence of VTE among patients with neuroepithelial tumor is actually higher than previously reported. Serial D-dimer sequential measurement and Doppler ultrasonography are effective methods for detection of VTE, because of low invasiveness and sensitivity/specificity. We would like to emphasize that early VTE detection using this combination enables appropriate treatment to avoid PE onset.

References

1. Heit JA, Silverstein MD, Mohr DN, Petterson TM, O'Fallon WM, Melton LJ III (2000) Risk factors for deep vein thrombosis and pulmonary embolism: a population-based case-control study. *Arch Intern Med* 160:809–815
2. Khorana AA (2003) Malignancy, thrombosis and Trousseau: the case for an eponym. *J Thromb Haemost* 1:2463–2465
3. Khorana AA, Francis CW, Culakova E, Kuderer NM, Lyman GH (2007) Frequency, risk factors, and trends for venous thromboembolism among hospitalized cancer patients. *Cancer* 110:2339–2346
4. Khorana AA, Francis CW, Culakova E, Kuderer NM, Lyman GH (2007) Thromboembolism is a leading cause of death in cancer patients receiving outpatient chemotherapy. *J Thromb Haemost* 5:632–634
5. Chew HK, Wun T, Harvey D, Zhou H, White RH (2006) Incidence of venous thromboembolism and its effect on survival among patients with common cancers. *Arch Intern Med* 166:458–464
6. Sorensen HT, Mellekjaer L, Olsen JH, Baron JA (1990) Prognosis of cancers associated with venous thromboembolism. *N Engl J Med* 343:1846–1850
7. Agnelli G, Piovella F, Buoncristiani P, Severi P, Pini M, D'Angelo A, Beltrametti C, Damiani M, Andrioli GC, Pugliese R,

- Iorio A, Brambilla G (1998) Enoxaparin plus compression stockings compared with compression stockings alone in the prevention of venous thromboembolism after elective neurosurgery. *N Engl J Med* 339:80–85
8. Semrad TJ, O'Donnell R, Wun T, Chew H, Harvey D, Zhou H, White RH (2007) Epidemiology of venous thromboembolism in 9489 patients with malignant glioma. *J Neurosurg* 106:601–608
 9. Stein PD, Beemath A, Meyers FA, Skaf E, Sanchez J, Olson RE (2006) Incidence of venous thromboembolism in patients hospitalized with cancer. *Am J Med* 119:60–68
 10. Mack WJ, Ducruet AF, Hickman ZL, Kalyvas JT, Cleveland JR, Mocco J, Schmidt M, Mayer SA, Connolly ES Jr (2008) Doppler ultrasonography screening of poor-grade subarachnoid hemorrhage patients increases the diagnosis of deep venous thrombosis. *Neurol Res* 9:889–892
 11. Becker DM, Philbrick JT, Abbitt PL (1989) Real-time ultrasonography for the diagnosis of lower extremity deep venous thrombosis. The wave of the future? *Arch Intern Med* 8:1731–1734
 12. Cogo A, Lensing AW, Wells P, Prandoni P, Buller HR (1995) Noninvasive objective tests for the diagnosis of clinically suspected deep-vein thrombosis. *Haemostasis* 1–2:27–39
 13. Gottlieb RH, Widjaja J, Tian L, Rubens DJ, Voci SL (1999) Calf sonography for detecting deep venous thrombosis in symptomatic patients: experience and review of the literature. *J Clin Ultrasound* 8:415–420
 14. Kassai B, Boissel JP, Cucherat M, Sonie S, Shah NR, Leizorovicz A (2004) A systematic review of the accuracy of ultrasound in the diagnosis of deep venous thrombosis in asymptomatic patients. *Thromb Haemost* 4:655–666
 15. Kearon C, Julian JA, Newman TE, Ginsberg JS (1998) Noninvasive diagnosis of deep venous thrombosis. *McMaster Diagnostic Imaging Practice Guidelines Initiative*. *Ann Intern Med* 8:663–677
 16. Mustafa BO, Rathbun SW, Whitsett TL, Raskob GE (2002) Sensitivity and specificity of ultrasonography in the diagnosis of upper extremity deep vein thrombosis: a systematic review. *Arch Intern Med* 4:401–404
 17. Segal JB, Eng J, Tamariz LJ, Bass EB (2007) Review of the evidence on diagnosis of deep venous thrombosis and pulmonary embolism. *Ann Fam Med* 5:63–73
 18. Wells PS, Lensing AW, Davidson BL, Prins MH, Hirsh J (1995) Accuracy of ultrasound for the diagnosis of deep venous thrombosis in asymptomatic patients after orthopedic surgery. A meta-analysis. *Ann Intern Med* 1:47–53
 19. White RH, McGahan JP, Daschbach MM, Hartling RP (1989) Diagnosis of deep-vein thrombosis using duplex ultrasound. *Ann Intern Med* 111:297–304
 20. Prisco D, Grifoni E (2009) The role of D-dimer testing in patients with suspected venous thromboembolism. *Semin Thromb Hemost* 35:50–59
 21. Brown MD, Rowe BH, Reeves MJ, Birmingham JM, Goldhaber SZ (2002) The accuracy of the enzyme-linked immunosorbent assay D-dimer test in the diagnosis of pulmonary embolism: a meta-analysis. *Ann Emerg Med* 2:133–144
 22. Brown MD, Lau J, Nelson RD, Kline JA (2003) Turbidimetric D-dimer test in the diagnosis of pulmonary embolism: a meta-analysis. *Clin Chem* 11:1846–1853
 23. Heim SW, Schectman JM, Siadaty MS, Philbrick JT (2004) D-dimer testing for deep venous thrombosis: a metaanalysis. *Clin Chem* 7:1136–1147
 24. Kobayashi T (2004) [Pulmonary thromboembolism. Deep vein thrombosis (venous thromboembolism)]. *Acta Obstet Gynaecol Jpn* 56:382–391
 25. Stein PD, Hull RD, Patel KC, Olson RE, Ghali WA, Brant R, Biel RK, Bharadia V, Kalra NK (2004) D-dimer for the exclusion of acute venous thrombosis and pulmonary embolism: a systematic review. *Ann Intern Med* 8:589–602
 26. Louis ND (ed) (2007) WHO classification of tumours of the central nervous system. IARC, Lyon
 27. Laporte S, Mismetti P, Décousus H, Uresandi F, Otero R, Lobo JL, Monreal M et al (2008) Clinical predictors for fatal pulmonary embolism in 15,520 patients with venous thromboembolism: findings from the Registro Informatizado de la Enfermedad Trombo-Embolica venosa (RIETE) Registry. *Circulation* 117:1711–1716
 28. Levitan N, Dowlati A, Remick SC, Tahsildar HI, Sivinski LD, Beyth R, Rimm AA (1999) Rates of initial and recurrent thromboembolic disease among patients with malignancy versus those without malignancy. Risk analysis using Medicare claims data. *Medicine* 78:285–291
 29. Kawaguchi T, Kumabe T, Kanamori M, Yamashita Y, Sonoda Y, Watanabe M, Tominaga T (2009) [Venous thromboembolism in patients with malignant glioma]. *Jpn J Neurosurg* 18:294–299
 30. Brandes AA, Scelzi E, Salmistraro G, Ermani M, Carollo C, Berti F, Zampieri P, Baiocchi C, Fiorentino MV (1997) Incidence of risk of thromboembolism during treatment high-grade gliomas: a prospective study. *Eur J Cancer* 33:1592–1596
 31. Simanek R, Vormittag R, Hassler M, Roessler K, Schwarz M, Zielinski C, Pabinger I, Marosi C (2007) Venous thromboembolism and survival in patients with high-grade glioma. *Neuro-oncology* 9:89–95
 32. Ay C, Vormittag R, Dunkler D, Simanek R, Chiriach AL, Drach J, Quehenberger P, Wagner O, Zielinski C, Pabinger I (2009) D-dimer and prothrombin fragment 1 + 2 predict venous thromboembolism in patients with cancer: results from the Vienna Cancer and Thrombosis Study. *J Clin Oncol* 27:4124–4129
 33. Eichinger S, Minar E, Bialonczyk C, Hirschl M, Quehenberger P, Schneider B, Weltermann A, Wagner O, Kyrle PA (2003) D-dimer levels and risk of recurrent venous thromboembolism. *JAMA* 290:1071–1074
 34. Palareti G, Legnani C, Cosmi B, Guazzaloca G, Pancani C, Coccheri S (2002) Risk of venous thromboembolism recurrence: high negative predictive value of D-dimer performed after oral anticoagulation is stopped. *Thromb Haemost* 87:7–12
 35. Palareti G, Legnani C, Cosmi B, Valdré L, Lunghi B, Bernardi F, Coccheri S (2003) Predictive value of D-dimer test for recurrent venous thromboembolism after anticoagulation withdrawal in subjects with a previous idiopathic event and in carriers of congenital thrombophilia. *Circulation* 108:313–318
 36. Kirwan CC, McDowell G, McCollum CN, Kumar S, Byrne GJ (2008) Early changes in the haemostatic and procoagulant systems after chemotherapy for breast cancer. *Br J Cancer* 99:1000–1006
 37. Satoh T, Matsumoto K, Uno K, Sakurai M, Okada S, Onuki M, Minaguchi T, Tanaka YO, Homma S, Oki A, Yoshikawa H (2008) Silent venous thromboembolism before treatment in endometrial cancer and the risk factors. *Br J Cancer* 99:1034–1039
 38. Ray WZ, Strom RG, Blackburn SL, Ashley WW, Sicard GA, Rich KM (2009) Incidence of deep venous thrombosis after subarachnoid hemorrhage. *J Neurosurg* 110:1010–1014
 39. Seidel AC, Cavalheri G Jr, Miranda F Jr (2008) The role of duplex ultrasonography in the diagnosis of lower-extremity deep vein thrombosis in non-hospitalized patients. *Int Angiol* 5:377–384
 40. McQueen AS, Elliott ST, Keir MJ (2009) Ultrasonography for suspected deep vein thrombosis: how useful is single-point augmentation? *Clin Radiol* 2:148–155
 41. Agnelli G, Radicchia S, Nenci GG (1995) Diagnosis of deep vein thrombosis in asymptomatic high-risk patients. *Haemostasis* 25:40–48

42. Nurmohamed MT, van Riel AM, Henkens CM, Koopman MM, Que GT, d'Azemar P, Büller HR, ten Cate JW, Hoek JA, van der Meer J, van der Heul C, Turpie AG, Haley S, Sicurella A, Gent M (1996) Low molecular weight heparin and compression stockings in the prevention of venous thromboembolism in neurosurgery. *Thromb Haemost* 75:233–238
43. Collen JF, Jackson JL, Shorr AF, Moores LK (2008) Prevention of venous thromboembolism in neurosurgery: a metaanalysis. *Chest* 134:237–249
44. Danish SF, Burnett MG, Ong JG, Sonnad SS, Maloney-Wilensky E, Stein SC (2005) Prophylaxis for deep venous thrombosis in craniotomy patients: a decision analysis. *Neurosurgery* 56:1286–1292
45. Seinturier C, Bosson JL, Colonna M, Imbert B, Carpentier PH (2005) Site and clinical outcome of deep vein thrombosis of the lower limbs: an epidemiological study. *J Thromb Haemost* 3:1362–1367

Regression of recurrent glioblastoma infiltrating the brainstem after convection-enhanced delivery of nimustine hydrochloride

Case report

RYUTA SAITO, M.D., PH.D.,¹ YUKIHIKO SONODA, M.D., PH.D.,¹
TOSHIHIRO KUMABE, M.D., PH.D.,¹ KEN-ICHI NAGAMATSU, M.D., PH.D.,¹
MIKA WATANABE, M.D., PH.D.,² AND TEIJI TOMINAGA, M.D., PH.D.¹

Departments of ¹Neurosurgery and ²Pathology, Tohoku University Graduate School of Medicine, Sendai, Miyagi, Japan

This 13-year-old boy with a history of cranial irradiation for the CNS recurrence of acute lymphocytic leukemia developed a glioblastoma in the right cerebellum. Resection and chemo- and radiotherapy induced remission of the disease. However, recurrence was noted in the brainstem region 8 months later. Because no effective treatment was available for this recurrent lesion, the authors decided to use convection-enhanced delivery (CED) to infuse nimustine hydrochloride. On stereotactic insertion of the infusion cannula into the brainstem lesion, CED of nimustine hydrochloride was performed with real-time MR imaging to monitor the co-infused chelated gadolinium. The patient's preinfusion symptom of diplopia disappeared after treatment. Follow-up MR imaging revealed the response of the tumor. The authors report on a case of recurrent glioblastoma infiltrating the brainstem that regressed after CED of nimustine hydrochloride. (DOI: 10.3171/2011.2.PEDS10407)

KEY WORDS • convection-enhanced delivery • glioblastoma • brainstem • nimustine hydrochloride • gadolinium

GLIOMAS diffusely affecting the brainstem have 2 different origins: one is the so-called brainstem glioma, and the other involves infiltration from gliomas originating in surrounding structures. Brainstem gliomas account for approximately 20% of all CNS tumors among children younger than 15 years of age. Among adults, brainstem gliomas are less common but have been reported in individuals up to the age of 70 years. Surgery no longer plays a role in diffuse brainstem glioma treatment. Meaningful resection is not possible, as the diffuse tumor is interwoven within white matter tracts traversing the brainstem, and resection does not confer a survival advantage.^{4,14} Radiotherapy was previously the recommended treatment for all brainstem gliomas, leading to transient improvements in neurological function and a progression-free survival benefit, but it does not

improve overall survival.⁵ Currently, there is little, if any, evidence to suggest that chemotherapy has affected the outcome in patients with diffuse brainstem gliomas.^{4,7} Consequently, the prognosis for diffuse brainstem glioma is very poor, with a median survival of less than 1 year. The median onset of disease progression following radiation is often less than 6 months, median survival is approximately 10 months, and less than 10% of patients are alive at 2 years.^{5,6} Gliomas originating from surrounding structures such as the thalamus or cerebellum also infiltrate the brainstem, often at the time of recurrence. In this setting, it is more complicated because radiotherapy has already been administered in many cases at the time of initial therapy. Therefore, novel treatment modalities are required.

In the present report, we describe a case of recurrent glioblastoma affecting the brainstem that regressed after local ACNU-based chemotherapy. The local chemotherapy was administered using CED, aided by real-time MR imaging monitoring.^{1–3,8,11,12}

Abbreviations used in this paper: ACNU = nimustine hydrochloride; CED = convection-enhanced delivery; Gd-DOTA = gadoterate meglumine.

Case Report

History. This 13-year-old boy developed truncal and right cerebellar ataxia, and he visited the department of pediatrics at our hospital in October 2008. He had a history of acute lymphocytic leukemia (French-American-British Class L1) and underwent chemotherapy at the age of 2 years. Recurrent disease in his testis and CNS was detected when he was 5 and 8 years of age, respectively. Both recurrent lesions were treated with combined chemo- and radiotherapy including 18-Gy whole-brain and whole-spine irradiation at 8 years of age. After these treatments, complete remission of the acute lymphocytic leukemia was achieved without any systemic or neurological deficits. However, in October 2008, T2-weighted MR imaging of the brain revealed a massive high-intensity lesion in the right cerebellar hemisphere (Fig. 1A). Contrast-enhanced T1-weighted MR imaging revealed spotty enhancement within the lesion (Fig. 1B). Magnetic resonance spectroscopy detected an elevated choline peak in the lesion. With a diagnosis of malignant glioma, he was referred to our department.

Treatment. The tumor was subtotally resected in November 2008 (Fig. 1C and D). After surgery, the patient underwent local radiotherapy (50 Gy) and concomitant temozolomide therapy. Exhibiting just slight ataxia, he was discharged from the hospital to home and enjoyed his school life until May 2009 (Fig. 1E and F). During this period, temozolomide-based chemotherapy was continued on an outpatient basis. On follow-up outpatient MR imaging in June 2009, slight enhancement was noted in the brainstem (Fig. 2A). Considering a differential diagnosis of tumor recurrence and radiation necrosis, we conducted

further examinations. A methionine-based PET study revealed a high uptake (maximal standardized uptake value = 4.2) (Fig. 2B), suggesting a tumor recurrence, and MR images obtained simultaneously depicted the enlargement of the enhanced tumor (Fig. 2C). At this point, we decided to perform CED of ACNU. During the preparation period of only 16 days, we observed additional enlargement of the enhanced tumor (Fig. 2D). The patient developed diplopia due to right-side medial-longitudinal-fasciculus syndrome. After planning the route for the catheter (iPlan stereotactic software, Brainlab), an 18-gauge 30-cm single-lumen central venous catheter (UNITIKA) was inserted via the left frontal lobe with stereotactic assistance (Fig. 3A–C). Ni-mustine hydrochloride solution, which contained 0.25 mg/ml of ACNU and 1 mM Gd-DOTA in saline, was infused over 2.5 days through the inserted catheter, using the CED method. Briefly, using a microinfusion pump, the infusion rate was controlled and gradually increased from 1.0 to 5.0 μ l/min, resulting in a total infusion of 7020 μ l after 2.5 days. Oral temozolomide at 200 mg/m²/day was used simultaneously for 5 sequential days starting from the day of catheter insertion. Intravenous dexamethasone was also used during infusion. Magnetic resonance images were obtained during and after infusion. Noncontrast T1-weighted MR imaging revealed the delivery of Gd-DOTA that was mixed in the infusion solution (Fig. 3D–G). The volume of distribution was plotted against the volume of infusion (Fig. 3H). We calculated the volume of distribution as the volume of distribution from MR images containing at least 10% of the total increase in signal intensity due to the addition of contrast agent as reported previously.¹³ The images in Fig. 4 (A–D) demonstrate the relationship of the tumor and distribution of Gd-DOTA at the end of

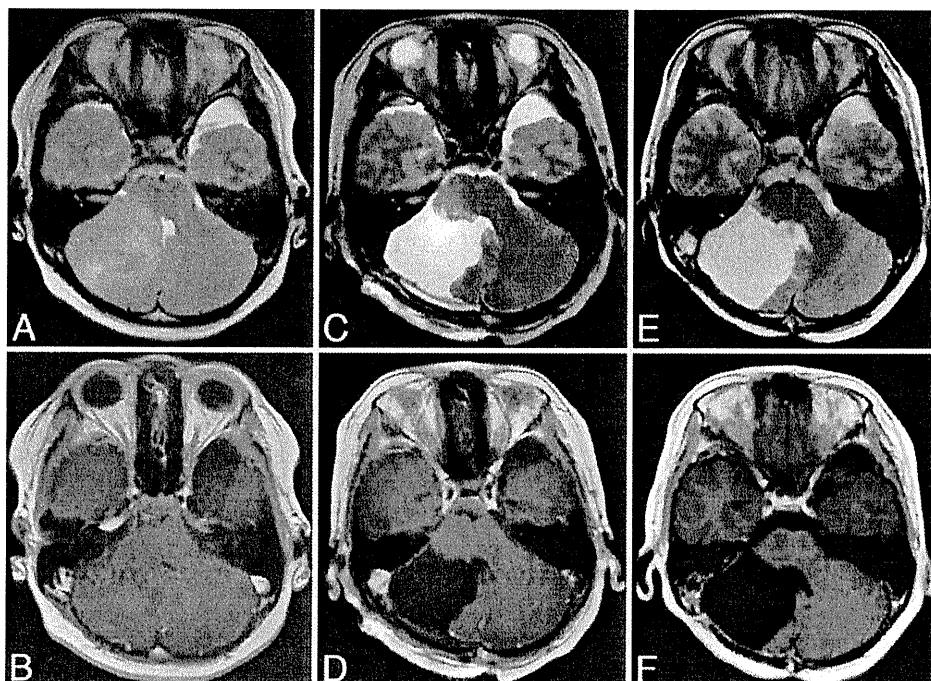


FIG. 1. Axial T2-weighted (A, C, and E) and contrast-enhanced T1-weighted (B, D, and F) MR images obtained at diagnosis in October 2008 (A and B), after tumor resection (C and D), and at follow-up in May 2009 (E and F).

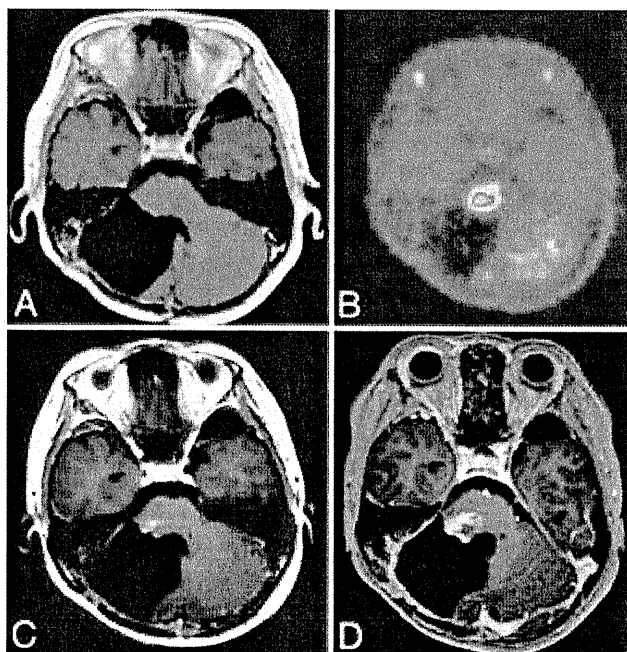


FIG. 2. Axial contrast-enhanced T1-weighted MR images obtained in June 2009 when recurrence in the brainstem was suspected (A), 6 days later (C) obtained together with a methionine-based PET scan (B), and 16 days later just before treatment CED (D).

CED. During the infusion, when infusion reached 2000 μ l, slight aggravation of right-side medial-longitudinal-fasciculus syndrome was observed. Development of mild right hemiparesis was noted 4 days after the termination of infusion, which fully recovered within a week. On a diffusion-weighted MR image obtained when hemiparesis was recognized, we noted a spotty high-intensity lesion in the left corona radiata (Fig. 4E). As Gd-DOTA was also found at this site in the image obtained at the end of infusion

(Fig. 4F), we considered this to represent a side effect of the delivered ACNU. Otherwise, the clinical course after CED was uneventful. The diplopia and right hemiparesis resolved. The patient returned to normal school life with the continuation of monthly temozolomide. Contrast-enhanced T1-weighted MR imaging revealed the shrinkage of the brainstem lesion (Fig. 5). Unfortunately in December 2009, the patient was readmitted to our hospital with the rapid progression of multiple disseminated diseases. In late January 2010, he died.

Discussion

We have been working toward the CED of ACNU to treat malignant gliomas. In our first article published in 2007, we demonstrated the efficacy of ACNU in a rodent intracranial xenograft tumor model.¹⁸ The subsequent publication demonstrated the efficacy of combination therapy using CED of ACNU and systemic temozolomide.¹⁹ We then concluded a toxicity study in nonhuman primates (unpublished data). Histological examination revealed minimum tissue damage after a 1-mg/ml infusion of ACNU, which was the safety dose detected in our previous rodent study. Based on these results, we started a pilot clinical study in 2008 on the CED of ACNU in patients with recurrent high-grade glioma after being granted approval from our institutional ethical committee. To treat recurrent high-grade gliomas, we used a mixture of ACNU and Gd-DOTA in CED. Starting from the day of infusion, temozolomide was also given orally for 5 consecutive days according to the protocol for recurrent disease. The present case was a patient involved in the study.

The treatment of a recurrent glioma affecting the brainstem is challenging. No effective therapy is available for patients in whom chemo- and radiotherapy have already been given for the initial disease. In the present case, the rapid progression of recurrent disease was detected on

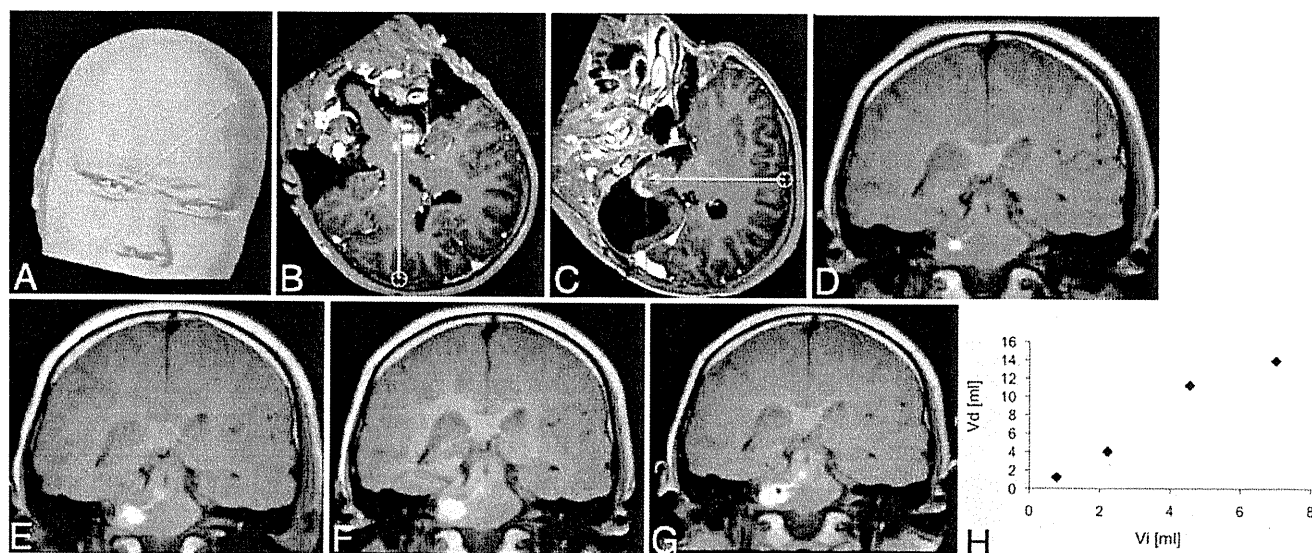


FIG. 3. A–C: Route of the catheter tract developed. D–G: Coronal T1-weighted MR images obtained during the CED of ACNU. The images were acquired when the infusion volumes were 780, 2220, 4560, and 7020 μ l, respectively. H: Volume of distribution (Vd) was plotted against volume of infusion (Vi) at 4 different time points.

Convection-enhanced delivery in recurrent brainstem glioblastoma

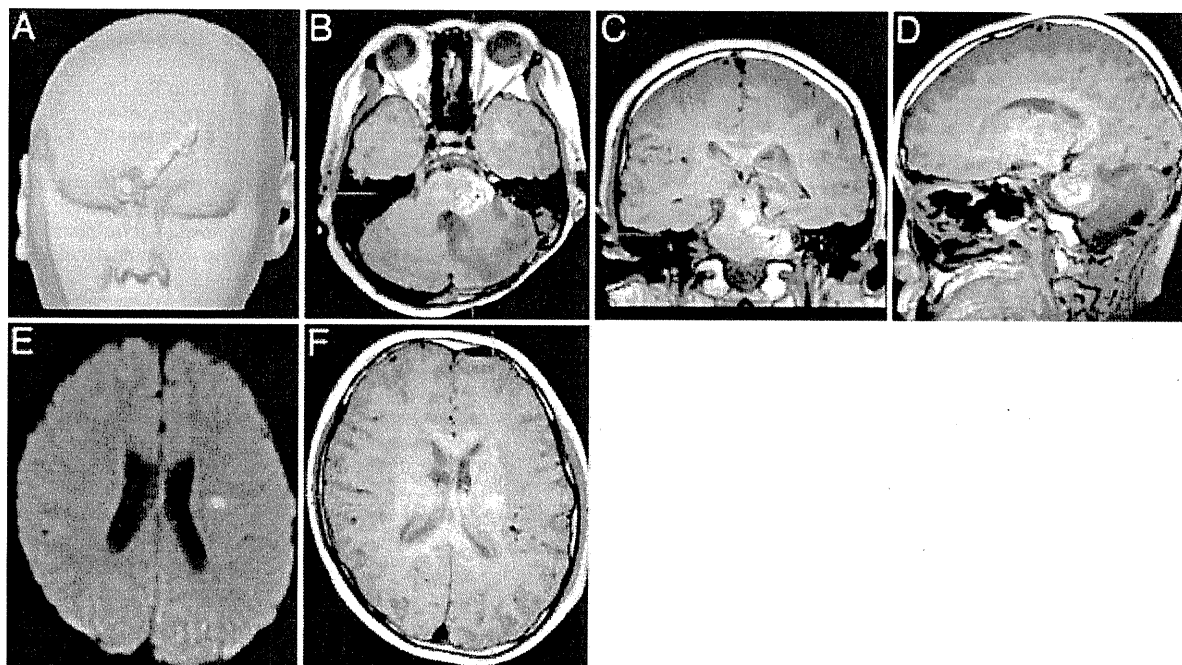


FIG. 4. Relationship between the enhanced tumor mass and distribution of CED Gd-DOTA. **A–D and F:** Images produced using the iPlan stereotactic software. The contrast-enhanced T1-weighted MR image are overlapped with the T1-weighted MR images obtained at the end of CED. The tumor is indicated by the *red* and the distribution of Gd-DOTA by *yellow*. The images in **A–D** demonstrate the relationship between the tumor and distribution of Gd-DOTA at the end of CED. Diffusion-weighted MR images, obtained when the patient developed mild right hemiparesis (**E**), showing a high-intensity lesion in the left corona radiata where there was a reflux of infused Gd-DOTA at the end of infusion (**F**).

MR imaging together with the rapid deterioration of diplopia. Methionine-based PET scanning detected a region of high uptake corresponding to the brainstem lesion, which suggested “recurrence” rather than radiation necrosis. We observed that CED of ACNU demonstrated the efficacy against this lesion. Regression of the lesion was documented together with the disappearance of diplopia. Although dissemination developed 5 months after CED, our patient was able to resume his school life until then. An important motivation for the development of CED has been the desire to offer a new treatment to children with diffuse pontine gliomas.^{9,10,17,20,21} In the present case the patient did not have diffuse pontine glioma, but the condition treated is similar. Thus, results in this case indicate a promise for future development of this delivery strategy.

Visualization of drug distribution during CED is also of importance in the future development of CED.^{8–13,15,16} The Gd-DOTA used in this study provided important information on drug delivery. Although it is not clear if the Gd-DOTA distribution directly reflects that of ACNU, there were findings that suggested a similarity in the distribution. Magnetic resonance imaging detected the backflow of Gd-DOTA through the catheter tract. The backflow was detected at the catheter tract penetrating the corona radiata of the left hemisphere. During infusion, we were anxious about this because, if the distribution of ACNU was the same as that of Gd-DOTA, this might cause some damage to the left corona radiata. Actually, the patient developed mild right hemiparesis after infusion. On diffusion-weighted MR imaging, performed when hemiparesis was

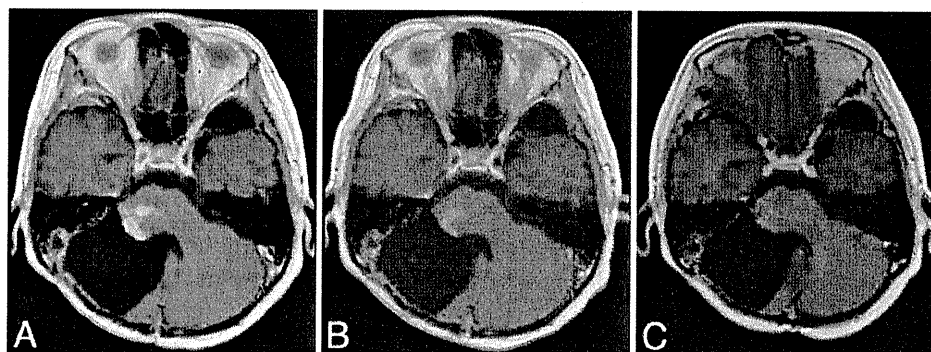


FIG. 5. Axial contrast-enhanced T1-weighted MR images obtained 1 week after CED (**A**), 1 month after CED (**B**), and 3 months after CED (**C**).

recognized, we observed a spotty high-intensity lesion in the left corona radiata. Fortunately, this symptom fully resolved soon after termination of the CED. However, this suggested the importance of monitoring the drug distribution during CED.

Based on these experiences, we are now planning a Phase I study on the MR imaging-monitored CED of ACNU for recurrent brainstem gliomas. Although the treatment of this disease is challenging, the present case suggests the possibility of using CED against this devastating disease. We can only treat localized disease with CED, and we still need to develop an effective treatment against disseminated disease. However, localized disease should be cured beforehand. Together with imaging guidance, this platform of therapy may provide an alternative therapeutic strategy to brainstem gliomas in the future.^{13,15}

Conclusions

The present case of recurrent glioblastoma affecting the brainstem suggests the efficacy of local chemotherapy aided by CED. Regression of the enhanced tumor as well as symptoms was achieved even with the recurrent, rapidly progressing disease. Although the patient finally died of disseminated disease, the CED of ACNU facilitated local control of the disease even in the brainstem region. Based on these experiences, we are now preparing a Phase I study on the MR imaging-monitored CED of ACNU for recurrent brainstem gliomas.

Disclosure

The authors report no conflict of interest concerning the materials or methods used in this study or the findings specified in this paper.

Author contributions to the study and manuscript preparation include the following. Author contributions to the study and manuscript preparation include the following. Conception and design: Saito. Acquisition of data: Saito, Sonoda, Kumabe, Nagamatsu, Watanabe. Analysis and interpretation of data: Saito, Sonoda, Kumabe, Nagamatsu. Drafting the article: Saito. Critically revising the article: Sonoda, Kumabe, Watanabe. Reviewed final version of the manuscript and approved it for submission: all authors. Study supervision: Tominaga.

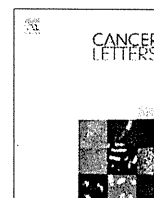
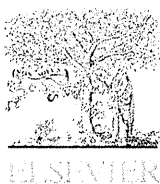
References

- Degen JW, Walbridge S, Vortmeyer AO, Oldfield EH, Lonser RR: Safety and efficacy of convection-enhanced delivery of gemcitabine or carboplatin in a malignant glioma model in rats. *J Neurosurg* **99**:893–898, 2003
- Ding D, Kanaly CW, Bigner DD, Cummings TJ, Herndon JE II, Pastan I, et al: Convection-enhanced delivery of free gadolinium with the recombinant immunotoxin MR1-1. *J Neurooncol* **98**:1–7, 2010 (Erratum in *J Neurooncol* **98**:9, 2010)
- Ding D, Kanaly CW, Cummings TJ, Li JE, Raghavan R, Sampson JH: Long-term safety of combined intracerebral delivery of free gadolinium and targeted chemotherapeutic agent PRX321. *Neurol Res* [epub ahead of print], 2009
- Donaldson SS, Laningham F, Fisher PG: Advances toward an understanding of brainstem gliomas. *J Clin Oncol* **24**:1266–1272, 2006
- Frazier JL, Lee J, Thomale UW, Noggle JC, Cohen KJ, Jallo GI: Treatment of diffuse intrinsic brainstem gliomas: failed approaches and future strategies. A review. *J Neurosurg Pediatr* **3**:259–269, 2009
- Freeman CR, Farmer JP: Pediatric brain stem gliomas: a review. *Int J Radiat Oncol Biol Phys* **40**:265–271, 1998
- Jalali R, Raut N, Arora B, Gupta T, Dutta D, Munshi A, et al: Prospective evaluation of radiotherapy with concurrent and adjuvant temozolomide in children with newly diagnosed diffuse intrinsic pontine glioma. *Int J Radiat Oncol Biol Phys* **77**:113–118, 2010
- Lonser RR, Schiffman R, Robison RA, Butman JA, Quezado Z, Walker ML, et al: Image-guided, direct convective delivery of glucocerebrosidase for neuronopathic Gaucher disease. *Neurology* **68**:254–261, 2007
- Lonser RR, Walbridge S, Garmestani K, Butman JA, Walters HA, Vortmeyer AO, et al: Successful and safe perfusion of the primate brainstem: in vivo magnetic resonance imaging of macromolecular distribution during infusion. *J Neurosurg* **97**:905–913, 2002
- Lonser RR, Warren KE, Butman JA, Quezado Z, Robison RA, Walbridge S, et al: Real-time image-guided direct convective perfusion of intrinsic brainstem lesions. Technical note. *J Neurosurg* **107**:190–197, 2007
- Mardor Y, Last D, Daniels D, Shneur R, Maier SE, Nass D, et al: Convection-enhanced drug delivery of interleukin-4 Pseudomonas exotoxin (PRX321): increased distribution and magnetic resonance monitoring. *J Pharmacol Exp Ther* **330**:520–525, 2009
- Murad GJ, Walbridge S, Morrison PF, Szerlip N, Butman JA, Oldfield EH, et al: Image-guided convection-enhanced delivery of gemcitabine to the brainstem. *J Neurosurg* **106**:351–356, 2007
- Nguyen TT, Pannu YS, Sung C, Dedrick RL, Walbridge S, Brechbiel MW, et al: Convective distribution of macromolecules in the primate brain demonstrated using computerized tomography and magnetic resonance imaging. *J Neurosurg* **98**:584–590, 2003
- Pierre-Kahn A, Hirsch JF, Vinchon M, Payan C, Sainte-Rose C, Renier D, et al: Surgical management of brain-stem tumors in children: results and statistical analysis of 75 cases. *J Neurosurg* **79**:845–852, 1993
- Saito R, Bringas JR, McKnight TR, Wendland MF, Mamot C, Drummond DC, et al: Distribution of liposomes into brain and rat brain tumor models by convection-enhanced delivery monitored with magnetic resonance imaging. *Cancer Res* **64**:2572–2579, 2004
- Saito R, Krauze MT, Bringas JR, Noble C, McKnight TR, Jackson P, et al: Gadolinium-loaded liposomes allow for real-time magnetic resonance imaging of convection-enhanced delivery in the primate brain. *Exp Neurol* **196**:381–389, 2005
- Sandberg DI, Edgar MA, Souweidane MM: Convection-enhanced delivery into the rat brainstem. *J Neurosurg* **96**:885–891, 2002
- Sugiyama S, Yamashita Y, Kikuchi T, Saito R, Kumabe T, Tominaga T: Safety and efficacy of convection-enhanced delivery of ACNU, a hydrophilic nitrosourea, in intracranial brain tumor models. *J Neurooncol* **82**:41–47, 2007
- Sugiyama S, Yamashita Y, Kikuchi T, Sonoda Y, Kumabe T, Tominaga T: Enhanced antitumor effect of combined-modality treatment using convection-enhanced delivery of hydrophilic nitrosourea with irradiation or systemic administration of temozolomide in intracranial brain tumor xenografts. *Neurol Res* **30**:960–967, 2008
- Thomale UW, Tyler B, Renard VM, Dorfman B, Guarnieri M, Haberl HE, et al: Local chemotherapy in the rat brainstem with multiple catheters: a feasibility study. *Childs Nerv Syst* **25**:21–28, 2009
- Yin D, Richardson RM, Fiandaca MS, Bringas J, Forsayeth J, Berger MS, et al: Cannula placement for effective convection-enhanced delivery in the nonhuman primate thalamus and brainstem: implications for clinical delivery of therapeutics. Laboratory investigation. *J Neurosurg* **113**:240–248, 2010

Manuscript submitted September 8, 2010.

Accepted February 11, 2011.

Address correspondence to: Ryuta Saito, M.D., Ph.D., Department of Neurosurgery, Tohoku University Graduate School of Medicine, 1-1 Seiryomachi, Aoba-ku, Sendai, 980-8574, Japan. email: ryuta@nsg.med.tohoku.ac.jp.



Local convection-enhanced delivery of chemotherapeutic agent transiently opens blood–brain barrier and improves efficacy of systemic chemotherapy in intracranial xenograft tumor model

Taigen Nakamura, Ryuta Saito*, Shin-ichiro Sugiyama, Yukihiro Sonoda, Toshihiro Kumabe, Teiji Tominaga

Department of Neurosurgery, Tohoku University Graduate School of Medicine, Sendai, Miyagi, Japan

ARTICLE INFO

Article history:

Received 15 February 2011

Received in revised form 2 June 2011

Accepted 12 June 2011

Keywords:

Convection-enhanced delivery

Local chemotherapy

Blood–brain barrier

Brain tumor

ACNU

ABSTRACT

Recently, local chemotherapy proved its efficacy against malignant gliomas. Under the hypothesis that local delivery of chemotherapeutic agents into the brain parenchyma induce opening of the blood–brain barrier (BBB), we evaluated the opening of BBB after convection-enhanced delivery of nimustine hydrochloride into the brain parenchyma. Local convection-enhanced delivery of nimustine hydrochloride transiently opened the BBB from about 7–12 days after delivery in normal rodent brain. Systemic chemotherapy during this period of BBB disruption had synergistic effects resulting in prolonged survival of tumor-bearing rats. The present strategy may provide a new approach for glioma chemotherapy.

© 2011 Elsevier Ireland Ltd. All rights reserved.

1. Introduction

Glioblastoma is the most common and most aggressive type of primary brain tumor. Approximately 3 in 100,000 people in the US and European countries are diagnosed with glioblastoma every year, and the median survival of a patient with glioblastoma is 15 months [1]. Only a minority of patients live longer than 3 years because therapies for the treatment of glioblastoma have only limited effectiveness despite the best efforts of researchers [2]. Post-surgical placement of small biodegradable polymer wafers designed to deliver carmustine (BCNU) directly into the resection cavity provides a survival benefit in patients with newly diagnosed and recurrent glioblastoma [3,4]. This procedure illustrates the therapeutic potential of extensive local chemotherapy against this devastating disease.

* Corresponding author. Address: Department of Neurosurgery, Tohoku University Graduate School of Medicine, 1-1 Seiryō-machi, Aoba-ku, Sendai, Miyagi 980-8574, Japan. Tel.: +81 22 717 7230; fax: +81 22 717 7233.

E-mail address: ryuta@nsg.med.tohoku.ac.jp (R. Saito).

The emergence of effective cancer chemotherapy is one of the major medical advances of the second half of the 20th century [5]. New lineups of chemotherapeutic agents and molecular targeted agents have been introduced to treat neoplasms. However, patients with gliomas fail to receive the benefits provided by most of these agents. Temozolomide is the only agent that has demonstrated therapeutic efficacy [6]. The properties of the blood–brain barrier (BBB), although compromised to some extent in glioblastomas, may be the reason for this failure [7]. Poor penetration of most anticancer drugs across the BBB and into the central nervous system is well documented. Even drugs that penetrate the BBB cannot reach adequate drug concentrations in brain-tumor tissue without causing systemic side effects [7]. Therefore, methods to transiently open this barrier have been extensively studied, including osmotic disruption using hyperosmotic shock [8], and biochemical disruption by administration of vasoactive substances [9].

Local drug delivery to the affected brain location should theoretically bypass the BBB, reduce systemic drug levels to minimize the side effects of chemotherapy, and provide

prolonged higher levels of intracerebral chemotherapeutic agents relative to those obtainable by systemic administration [7,10]. However, for many local drug-delivery technologies including simple intratumoral injection or polymer implantation, the ultimate efficacy depends on the diffusion of the drugs into the brain parenchyma. An important advance in local drug delivery is the development of convection-enhanced delivery (CED) [11]. This technique uses bulk flow to directly deliver small or large molecules to targeted sites in clinically significant volumes of tissue, resulting in improved volumes of distribution compared with simple diffusion techniques [10]. This technique is now being applied to deliver BCNU [12], topotecan [13], carboplatin, gemcitabine [14], and paclitaxel [15] to brain tumors, all with promising outcomes.

Recently, we have been investigating the CED of nimustine hydrochloride (ACNU) as a new strategy to effectively treat glioblastoma [16–18]. During our study, we observed a period when the brain treated with ACNU becomes enhanced on magnetic resonance imaging after intravenous administration of contrast agents, suggesting that the BBB becomes leaky after local administration of chemotherapeutic agent. In the present study, we tried to identify this leaky period, and investigated whether the efficacy of combination systemic chemotherapy was enhanced during this period.

2. Materials and methods

2.1. Pegylated (polyethylene glycol-coated) liposomal doxorubicin (PLD) and ACNU

PLD (Doxil; Alza Pharmaceuticals, Mountain View, CA) was obtained commercially. The commercial PLD solution contained 2 mg/mL of doxorubicin. ACNU was provided by Daiichi-Sankyo Co. Ltd. (Tokyo, Japan). Infusion solutions of ACNU were prepared by diluting ACNU in 0.9% NaCl solution to a concentration of 1 mg/mL.

2.2. Tumor cell line, animals, and intracranial xenograft technique

The 9 L rat gliosarcoma cells (American Type Culture Collection, Rockville, MD) were maintained as monolayers in a complete medium consisting of Eagle's minimal essential medium supplemented with 10% fetal bovine serum, non-essential amino acids, and 100 U/mL penicillin G. Cells were cultured at 37 °C in a humidified atmosphere consisting of 95% air and 5% CO₂. Male Sprague–Dawley rats weighting approximately 200 g were purchased from Charles-River Japan Laboratories (Tsukuba, Ibaraki, Japan). Male Fisher 344 rats weighting approximately 200 g were purchased from Kumagai-Shigeyasu Co., Ltd. (Sendai, Miyagi, Japan). All protocols used for the animal studies were approved by the Institute for Animal Experimentation of Tohoku University Graduate School of Medicine. To establish the intracranial xenograft tumor model, cells were harvested by trypsinization, washed once with Hanks' balanced salt solution without Ca²⁺ and Mg²⁺ (HBSS), and resuspended in HBSS for implantation. A cell

suspension containing 5×10^5 cells/10 μ L HBSS was used for implantation into the striatal region of the Fisher 344 rat brains. Under deep halothane anesthesia, rats were placed in a small-animal stereotactic frame (David Kopf Instrument, Tujunga, CA). A sagittal incision was made to expose the cranium followed by a burr hole in the skull located at 0.5 mm anterior and 3 mm lateral from the bregma using a small dental drill. Cell suspension (5 μ L) was injected over 2 min at a depth of 4.5 mm from the brain surface; after a 2-min wait, another 5 μ L was injected over 2 min at a depth of 4.0 mm; and after a final 2-min wait, the needle was removed and the wound was sutured.

2.3. Convection-enhanced delivery

CED with a volume of 20 μ L of ACNU or PBS was performed as described previously [19,20]. Briefly, the infusion system consisted of a reflux-free, step-design infusion cannula connected to a loading line (containing ACNU or PBS (GIBCO™ PBS; Life technologies Japan Ltd., Tokyo, Japan)) and an olive oil infusion line. A 1-mL syringe (filled with oil) mounted onto a micro-infusion pump (BeeHive; Bioanalytical Systems, West Lafayette, IN) regulated the flow of fluid through the system. Based on chosen coordinates, the infusion cannula was mounted onto stereotactic holders and guided to the target region of the brain through burr holes made in the skull. The following ascending infusion rates were applied to achieve 20 μ L infusion: 0.2 μ L/min (15 min) + 0.5 μ L/min (10 min) + 0.8 μ L/min (15 min).

2.4. Evaluation of toxicity

Three healthy male Sprague–Dawley rats weighing approximately 200 g received a single 20 μ L CED infusion of 1 mg/mL ACNU. Rats were monitored daily for survival, weekly weights, and general health. Rats were euthanized on the 60th day after the CED, and their brains were removed, fixed, subjected to paraffin sectioning (5 μ m), and stained with hematoxylin and eosin.

2.5. Volumetric evaluation of BBB disruption

Twenty normal male Fisher 344 rats weighting approximately 200 g received a single 20 μ L CED infusion of 1 mg/mL ACNU and were randomly assigned to five groups. In each group of four rats, 1 mL of 2% Evans blue solution (Sigma–Aldrich, Tokyo, Japan) in saline was administered through the tail veins at 3, 7, 12, 20, and 30 days after CED. Rats were euthanized 30 min after administration. After transcardial perfusion with NaCl solution, their brains were harvested, frozen with ice-cold isopentane, and cut into serial coronal sections (25 μ m) with a cryostat. Evans blue generates fluorescence under UV illumination, so the areas of brain section containing extravasated Evans blue were visualized using a fluorescence microscope, and a charged-coupled device camera with a fixed aperture was used to capture the image. The volumes of brain that contained extravasated Evans blue were calculated from these images.

2.6. Quantitative evaluation of BBB disruption

Twenty-four normal male Fisher 344 rats weighing approximately 200 g received a single 20 μ L CED infusion of 1 mg/mL ACNU. As for volumetric analysis, 1 mL of 4% Evans blue solution was administered to Fisher 344 rats 3 ($n = 9$), 7 ($n = 9$), and 30 ($n = 6$) days after CED. Rats were euthanized 30 min after Evans blue administration. After transcatheterial perfusion with NaCl solution, their brains were harvested. Extravasation of Evans blue in the hemispheres (3 mm anterior and 3 mm posterior from the CED point) was measured according to the method of Chan et al. [21,22]. After homogenization with 1 mL PBS, samples were centrifuged at 1000g for 30 min. Supernatants (0.7 mL) were taken, and an equal volume of 100% trichloroacetic acid was added to precipitate protein. The samples were allowed to stand overnight at 4 °C, and were then centrifuged at 1000g for 30 min. The absorbance of Evans blue at 610 nm was measured in the supernatants using a spectrophotometer. Evans blue content was expressed as μ g per hemisphere calculated against a standard.

2.7. Extravasation of PLD after CED in intracranial xenograft tumor model

Six male Fisher 344 rats with intracranial xenograft tumors were used for this study. Five days after tumor implantation, three rats received CED of ACNU (0.1 mg/mL, 20 μ L), and three rats received CED of 20 μ L PBS. Seven days after CED, all rats received bolus intravenous injections of 1 mL PLD solution (2.0 mg/mL) via the tail veins. Thirty minutes after PLD administration, rats were perfused transcatheterially with NaCl solution. Brains were harvested and frozen with ice-cold isopentane, and cut into serial coronal sections (25 μ m) with a cryostat. PLD generates fluorescence under UV illumination, so the areas of brain section containing extravasated PLD were visualized using a fluorescence microscope, and a charged-coupled device camera with a fixed aperture was used to capture the image. The same sections were then stained with hematoxylin and eosin.

2.8. Survival study using the intracranial xenograft model

Forty-two male Fisher 344 rats with intracranial xenograft tumors were randomly assigned to five groups as summarized in Table 1: (a) control group received CED of PBS ($n = 9$), (b) group received intravenous PLD administration after CED of PBS ($n = 9$), (c) group received CED of ACNU ($n = 8$), (d) group received intravenous PLD adminis-

tration after CED of ACNU ($n = 9$); and (e) group received CED of ACNU after intravenous PLD administration ($n = 7$). Five days after tumor cell implantation (Day 5), single CED infusions (20 μ L infusion of 1 mg/mL ACNU or PBS) were performed for groups (a, b, c, and d), and bolus intravenous injections of 400 μ L PLD (2.0 mg/mL) via the tail veins were performed for group (e). Seven days later (Day 12), bolus intravenous injections of 400 μ L PLD (2.0 mg/mL) via the tail veins were performed for groups (b, d, and e). Six days later (Day 18), bolus intravenous injections of 400 μ L PLD (2.0 mg/mL) via the tail veins were performed for groups (b and d), and CED infusions (20 μ L of 1 mg/mL ACNU) were performed for group (e). The dose of PLD used in this study was selected based on previous studies [23,24]. Survival was expressed as a Kaplan–Meier curve. Survival was compared between the treatment groups with a log-rank test.

3. Results

3.1. Negligible local toxicity of 1 mg/mL ACNU delivered via CED

CED infusion of 20 μ L ACNU at concentration of 1 mg/mL caused little local tissue damage when infused into normal rat hemisphere (Fig. 1), as previously reported [16,17]. Slight tissue damage was noted only at the needle tract without obvious tissue damage in the surrounding brain that received ACNU. Even at higher magnification, no strong inflammatory response or tissue necrosis was detected. No rat developed neurological deficit or lost their weight. This dose of ACNU (20 μ L of 1 mg/mL ACNU) was used throughout this study.

3.2. Extravasation of intravenous Evans blue 7 days after CED of ACNU

Although CED of ACNU caused little local tissue change as described above, leakage of intravenously infused 2% Evans blue solution was observed 7 days after CED of ACNU into the hemispheres of normal Fisher 344 rats. Representative brain sections are shown in Fig. 2A. Fluorescent microscopy detected Evans blue in the brain parenchyma indicating leakage from the BBB. In contrast, leakage of Evans blue was hardly observed 7 days after CED of PBS (Fig. 2B). Results were similar for all four rats tested.

3.3. Transient disruption of BBB after CED of ACNU

To test the time course of BBB disruption, leakage of intravenously infused Evans blue solution was evaluated 3, 7, 12, 20, and 30 days after CED of ACNU using fluorescent images. The leakage of Evans blue was small 3 days after CED, but became prominent from 7 to 12 days after CED, and then diminished (Fig. 3). Volumetric analysis of the fluorescent area confirmed the findings.

3.4. Quantitative analysis of transient disruption of BBB after CED of ACNU

Quantitative spectrophotometric analysis of Evans blue leakage through the disrupted BBB compared the amount of Evans blue in the brains of rats 3, 7, and 30 days after CED of ACNU. Brains of rats contained

Table 1

Five groups for survival study using the intracranial xenograft model.

Group	n	Day 0	Day 5	Day 12	Day 18
(a) Control	9	Implantation	PBS CED	PBS iv	PBS iv
(b) PLD iv	9	Implantation	PBS CED	PLD iv	PLD iv
(c) ACNU CED	8	Implantation	ACNU CED	PBS iv	PBS iv
(d) ACNU CED + PLD iv	9	Implantation	ACNU CED	PLD iv	PLD iv
(e) PLD iv + ACNU CED	7	Implantation	PLD iv	PLD iv	ACNU CED

Abbreviations: iv = intravenous, CED = convection-enhanced delivery, PLD = pegylated liposomal doxorubicin, PBS = phosphate buffered saline.

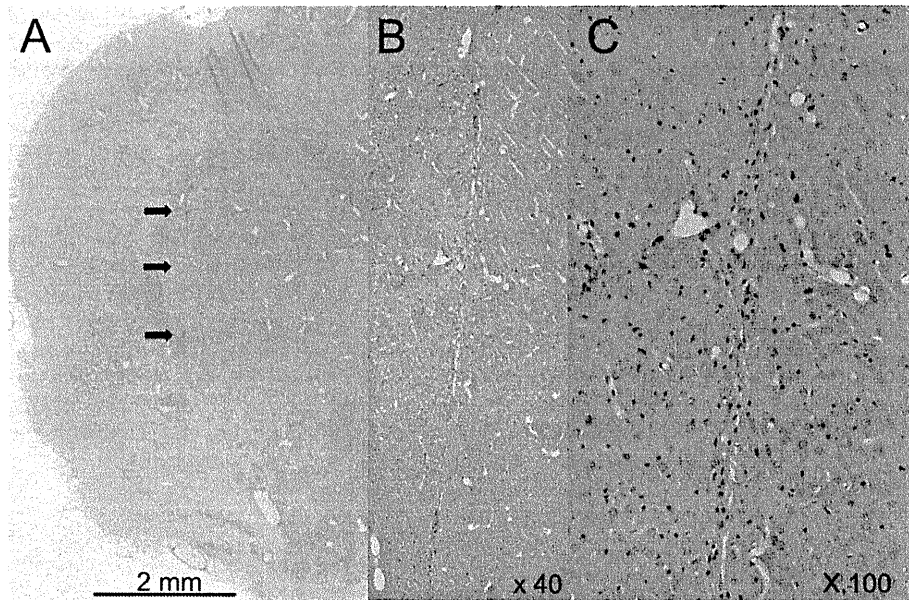


Fig. 1. Local tissue toxicity of ACNU administered via CED in the normal adult rat brain. Rat brains were treated with a single CED infusion of 20 μ L of 1.0 mg/mL ACNU. Representative hematoxylin and eosin sections from rats euthanized 30 days after CED. Rats showed no drug-induced damage (A). Arrows indicate the needle tract. Higher magnification of tissue around needle tract (B: $\times 40$, C: $\times 100$).

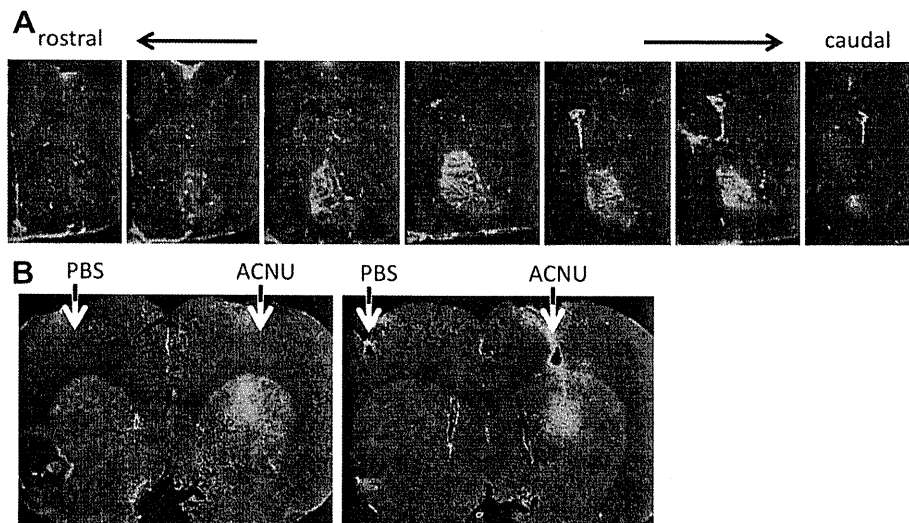


Fig. 2. Seven days after CED of ACNU into the hemisphere of normal Fisher 344 rats, 2% Evans blue solution was injected via the tail vein. Rats were euthanized 30 min after Evans blue administration. After transcardial perfusion with NaCl solution, their brains were harvested, frozen, and cut into serial coronal sections (25 μ m) with a cryostat. Brain sections were observed with a fluorescence microscope to detect the extravasation of Evans blue. Sequential brain sections at 500- μ m intervals from a representative rat are shown (A). Sequential brain sections at 500- μ m intervals of another rat that received tail vein injection of 2% Evans blue 7 days after CED of ACNU into one hemisphere and CED of PBS into the other hemisphere (B).

significantly higher amount of Evans blue 7 days after CED than on other days (Fig. 4), which confirmed the findings of the volumetric analysis.

3.5. Disruption of BBB after CED of ACNU in xenograft tumor model

Tumor vessels are usually more leaky than normal vessels. BBB disruption was evaluated in the intracranial xenograft tumor model. Seven days after CED of ACNU ($n = 3$) or PBS ($n = 3$), PLD was injected from the tail vein. Although mild leakage was observed in rats that received CED of PBS, leakage was more extensive in rats that received CED of ACNU (Fig. 5). One of three rats that received CED of ACNU harbored two separate tumors located just at the needle tract of ACNU infusion and at a dee-

per location probably not reached by infused ACNU. This enabled us to evaluate the efficacy of infused ACNU. Leakage of PLD was more prominent in the tumor located at the needle tract compared to the deeply located tumor. With the hypothesis that this leakage of PLD after CED of ACNU may benefit the survival of brain tumor xenografts, we conducted the following survival study.

3.6. Survival study

Survival study is summarized as a Kaplan–Meier curve (Fig. 6). CED of ACNU ($P = 0.017$; log-rank test) but not PLD ($P = 0.26$) prolonged the survival of tumor-bearing rats. Survival was improved when CED of ACNU

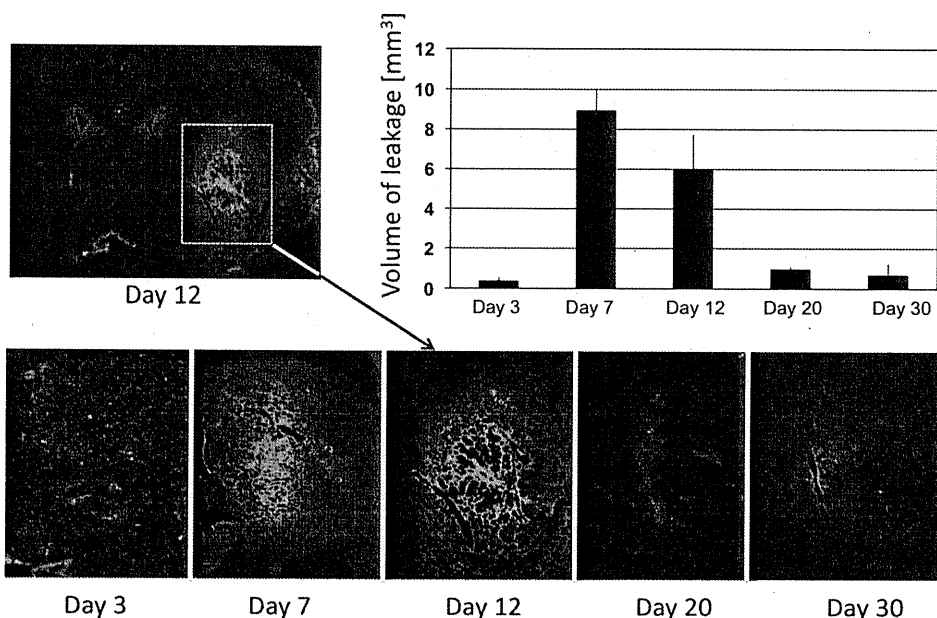


Fig. 3. Leakage of intravenously infused Evans blue solution 3, 7, 12, 20, and 30 days after CED of ACNU. Brains were processed as in Fig. 2 and observed under a fluorescence microscope. Representative image from rat brain that received Evans blue 12 days after CED (upper left). Lower images depict the magnified images of the boxed area from each day period. The fluorescence images were acquired under the same conditions. Volumetric analysis of the area that contained fluorescence from Evans blue (upper right). Bars at top of each column indicate the standard deviation.

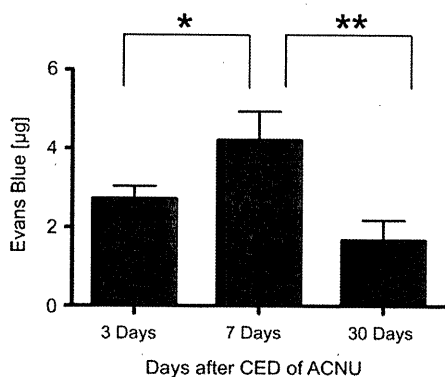


Fig. 4. Evans blue content in the brains of rats that received intravenous injection of 4% Evans blue solution 3, 7, and 30 days after CED of ACNU was measured using a spectrophotometer. Evans blue content was expressed as µg per hemisphere calculated against a standard. Bars at top of each column indicate the standard deviation. * $P=0.042$, ** $P=0.013$, Student t -test.

was given prior to PLD ($P=0.0001$; compared with control, $P=0.003$; compared with CED of ACNU alone), but not when PLD was given prior to CED of ACNU ($P=0.27$; compared with control). BBB disruption caused by CED of ACNU may be one reason for this improved survival.

4. Discussion

Our previous studies reported the safety and efficacy of CED of ACNU in the intracranial xenograft tumor model [16,17]. The present study confirmed that CED of 1 mg/mL ACNU produced no severe toxicity (Fig. 1). However, disruption of the BBB was observed. Qualitative eval-

uation revealed robust distribution of Evans blue in the normal rat hemisphere after intravenous administration, which was confirmed by quantitative evaluation.

Local chemotherapy can be effective against malignant gliomas, and CED can deliver drugs much more extensively into the target region, but may have some limitations. The vast majority of neoplastic cells in malignant gliomas are found within the tumor bed and within 2 cm of the enhanced borders, but migrating cells can be found several centimeters away from the tumor and even in the contralateral hemisphere [25]. Moreover, dissemination limits the survival of patients with locally well controlled malignant gliomas [26]. Therefore, effective local therapy should be administered together with effective systemic therapy. However, systemic chemotherapy is limited because 98% of small molecules and 100% of large molecules cannot cross the BBB [27]. Many promising agents including molecular targeted agents have not been as effective as expected.

In this context, our findings provide the rationale for combining local and systemic chemotherapy. The observed BBB disruption after local chemotherapy was reversible. Leakage was observed only between 1 and 2 weeks after delivery of ACNU. The exact mechanism for this transient disruption of the BBB is not clear, but slight disturbance of the BBB caused by chemotherapeutic agents is likely to recover fairly rapidly. In this study, delivery of intravenous Evans blue or PLD was augmented during this time window, but not later. Therefore, this transient dysfunction of the BBB gives a time window for effective delivery of systemic chemotherapeutic agents.

Drug delivery to brain tumors has been a controversial subject. Some researchers believe that the BBB is not

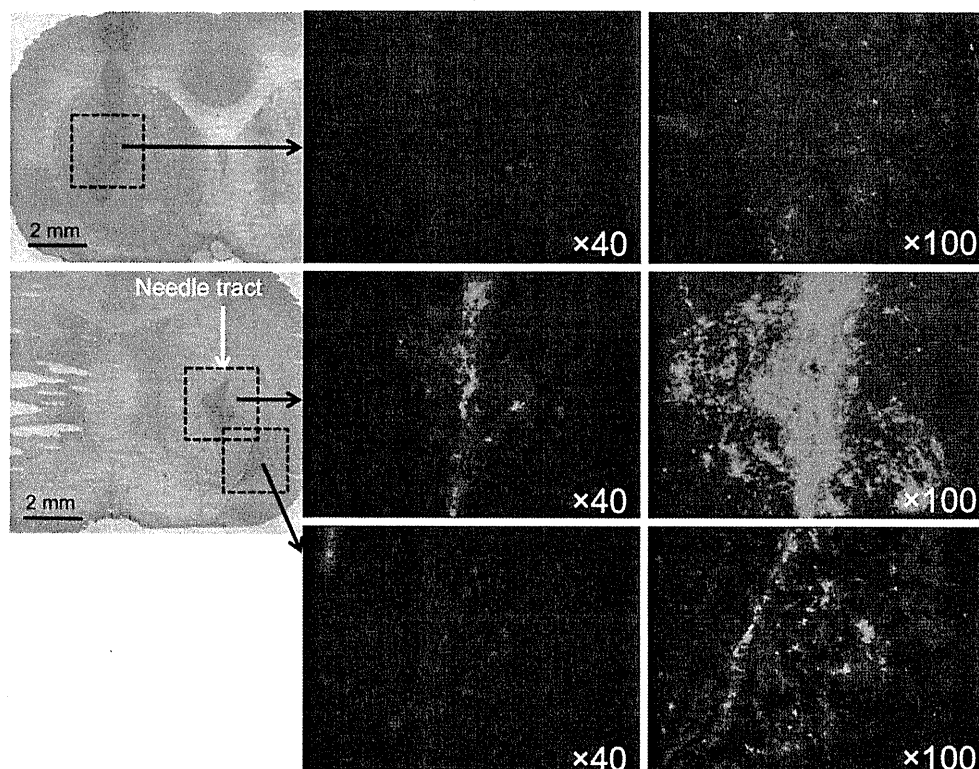


Fig. 5. Seven days after CED of ACNU ($n = 3$) or PBS ($n = 3$), PLD was injected via the tail vein. Although mild leakage was observed in rats that received CED of PBS (upper row), leakage was more extensive in rats that received CED of ACNU (middle and lower row). One of three rats that received CED of ACNU had two separate tumors, located just at the needle tract of ACNU infusion and at a deeper location probably not reached by infused ACNU. Leakage of PLD was more prominent in the tumor located at the needle tract (middle row) compared to the deeply located tumor (lower row).

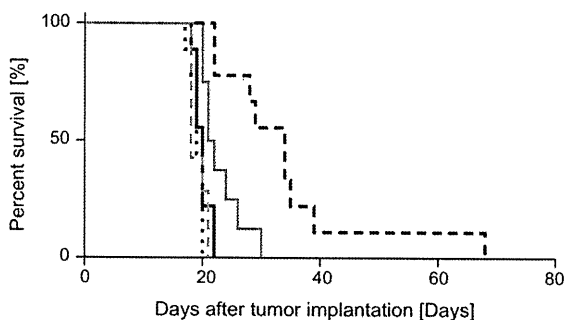


Fig. 6. Survival of the five groups expressed as a Kaplan–Meier curve. Black solid line, (a) control; black dotted line, (b) intravenous PLD; gray solid line, (c) CED of ACNU; black dashed line, (d) CED of ACNU plus intravenous PLD; and gray dashed line, (e) intravenous PLD plus CED of ACNU.

important, while others believe it is the major obstacle in treatment [28]. However, on the whole, the understanding is that the BBB and the blood–tumor barrier prevent drugs from reaching brain tumors in sufficient concentrations to kill the tumor cells [7]. In this study, we evaluated the leakage of PLD into the xenograft brain tumor model. Permeability of experimental gliomas is reported to be 10^4 – 10^5 higher than the normal brain if the molecular size of the agent is small enough [29]. Fluorescence from PLD was

observed in the tumors, but the fluorescence was obviously more intense after infusion of ACNU. The survival study also demonstrated the efficacy of the combination of ACNU CED and intravenous PLD, but only if intravenous PLD was given during the period of BBB disruption. This combination significantly prolonged survival of the tumor model rats if intravenous PLD was given 5 and 12 days after CED of ACNU. This efficacy was not observed if the agents were used in the opposite order. Moreover, the group treated by CED of ACNU following intravenous administration of PLD did not survive longer than the control group while the group treated by CED of ACNU had significantly longer survival than the control group. This may be because that xenografted tumors 18 days after implantation become too large to be treated by CED of $20 \mu\text{L}$ ACNU although intravenous PLD was given 5 and 12 days after implantation.

Many methods have been assessed to transiently disrupt the BBB for effective drug delivery to the central nervous system. Osmotic disruption such as hyperosmotic shock, and biochemical disruption induced by administration of vasoactive substances have been tested [8,9,27]. Tumor chemotherapy combined with these BBB opening agents seemed promising at first, but were abandoned because of the potential for structural brain damage in areas of BBB disruption. Compared with these strategies, the present method disrupts the BBB only at the site of drug